

Article

Prediction of Manufacturing Quality of Holes Based on a BP Neural Network

Anyuan Jiao ^{1,2} , Guofu Zhang ², Binghong Liu ² and Weijun Liu ^{3,*}

¹ School of Mechanical Engineering and Automation, Northeastern University, Shenyang 110819, China; jay@ustl.edu.cn

² School of Applied Technology, University of Science and Technology Liaoning, Anshan 114041, China; zhanggf@ustl.edu.cn (G.Z.); liubh@ustl.edu.cn (B.L.)

³ School of Mechanical Engineering, Shenyang University of Technology, Shenyang 110870, China

* Correspondence: liuwj@huiyuanrobot.com

Received: 31 December 2019; Accepted: 12 March 2020; Published: 20 March 2020



Abstract: In order to improve the manufacturing quality of holes ($\Phi 3$ – $\Phi 8$ mm) and to optimize the hole drilling process in T300 carbon fiber-reinforced plastic (CFRP) and 7050-T7 Al alloy stacks, a prediction model of multiple objective parameter optimization was proposed based on a back propagation (BP) neural network algorithm. Four parameters of feed rate, spindle speed, drilling diameter, and cushion plate were taken as the input layer parameters to study the manufacturing quality of holes in four stack types: CFRP/Al, Al/CFRP, Al/CFRP/Al, and CFRP/Al/CFRP. Delamination and tearing defects often appear in the drilling process; thus, a certain degree of defects in CFRP was selected as the output parameter, in an effort to build a prediction model of drilling quality. After the neural network model of the optimized hole-making process of an 8–14–1 three-layer topology was corrected by 170 steps, the error was reduced to 0.00016882, the regression fitting was 0.99978, and the fitting error of training samples was 10^{-2} – 10^{-5} . The prediction model of the number of defective holes provided basically similar results to the experimental data. This indicates that the prediction model based on a BP neural network has good prediction ability. Based on the prediction of parameters, verification tests were performed, and the number of defective holes in CFRP was reduced while the manufacturing quality of the holes was improved significantly; the qualified rate of manufactured holes reached 97%.

Keywords: neural network algorithms; CFRP; drilling; quality prediction

1. Introduction

Carbon fiber-reinforced plastic (CFRP) has several advantages such as light weight, high specific strength, corrosion resistance, and good vibration absorption. It is widely used in the aerospace, automotive, and civil engineering industries, among other fields [1]. Based on the orthogonal to oblique cutting transformation, a thermo-mechanical finite element (FE) model was established to simulate the conventional drilling and ultrasonic vibration drilling processes, and drilling-induced damage was predicted by Qiu et al. [2]. Shutao et al. [3] constructed a CFRP/Al three-dimensional drilling finite element simulation model by using the finite element software Abaqus. The tearing, delamination damage, burr formation characteristics, and mechanism of carbon fiber composites during CFRP/Al drilling were simulated. Dharan et al. [4] explored an intelligent control model for the processing of composite materials. A series of drilling tests were carried out on CFRP laminates by using machining centers, and the key process parameters under various cutting conditions were determined. Davim et al. [5] presented a new comprehensive approach to select cutting parameters for damage-free drilling in carbon fiber-reinforced epoxy composite material. Hybrid composites, composites with tough

thermoplastic resins, modified matrices, surface modification of fibers, translaminar reinforcements, and interlaminar modifications such as interleaving, short fiber reinforcement, and particle-based interlayer were discussed by Mubarak et al. [6]. Hocheng et al. [7] comprehensively analyzed the delamination of different types of bits, and the critical thrust at the beginning of the stratification was predicted and compared with the twist drill. Omar et al. [8] introduced a generic and improved model to simultaneously predict the conventional cutting forces along with three-dimensional (3D) surface topography during a side milling operation. An improved technique to calculate the instantaneous chip thickness was also presented. Kalla et al. [9] proposed a methodology for predicting the cutting forces by transforming specific cutting energies from orthogonal cutting to oblique cutting. The results showed that the method can predict the cutting forces in helical end milling of unidirectional and multidirectional composites, as well as over the entire range of fiber orientations from 0° to 180°. Karpat et al. [10] employed uncoated carbide and two diamond-coated carbide drills with different drill tip angles in drilling experiments of aerospace-quality thick fabric woven CFRP laminates. Chen et al. [11] used a staggered tool to mill carbon fiber, studied the influence of cutting radius on tool wear, found the influence of cutting radius on milling force and surface quality, and discussed the formation mechanism of three-dimensional surface topography.

The back propagation (BP) neural network algorithm is a new type of artificial intelligence technology, which achieved good results in performance prediction, process optimization, etc. Ugoenemuoh [12] proposed a robust design method for predicting the neural network model of a carbon fiber-reinforced epoxy resin (BMS 8-256) drilling layer, damage width, and hole surface roughness. The method was based on parametric analysis of the neural network model, using experimental design methods to accurately predict process-induced damage. Karnik et al. [13] focused on the effects of the drilling process parameters on the delamination behavior at the inlet of carbon fiber composites. An artificial neural network model with spindle speed, feed rate, and point angle as parameters was established, and high-speed drilling stratification analysis was carried out. The analysis demonstrated the advantage of using a higher speed to control stratification during drilling.

Based on the analysis of the above references, it can be seen that there were some studies on the prediction and analysis of the quality of hole-making, which mainly focused on the verticality of the deep holes, the roughness of the inner surface of the metal material, and the axial force of the composite material when drilling holes. The axial force of the composite material is an important factor that affects the defects of hole-making. These studies focus on predicting a single material and a single object. However, the aluminum alloy and CFRP stack material is the focus of this manuscript. Based on the BP neural network algorithm, the final drilling quality of the CFRP material is predicted and analyzed. Evaluation of the results can greatly reduce the probability of defective holes, as well as provide optimized solutions for efficient and high-quality hole-making of stack material.

2. The Plan of Hole Manufacturing

2.1. The Device of Hole Manufacturing

In this paper, the hole-making schematic was as shown in Figure 1. In order to ensure that there was no gap between the cushion plate and stacks, the C-clip was used to fasten the cushion plate and stacks. Similarly, in order to enable the stack material to withstand the sufficient drilling forces, a support block was placed underneath it. The box-type support block supports the surroundings of the stack material. The stacks were composed of 7050-T7 Al alloy with a thickness of 2 mm and T300 CFRP with a thickness of 3 mm. Then, a model with a of 8–14–1 three-layer topology was designed using the BP neural network algorithm. By means of learning, training, prediction, and verification, the quality on manufacturing holes could be predicted, and the final optimized hole-making process was verified.

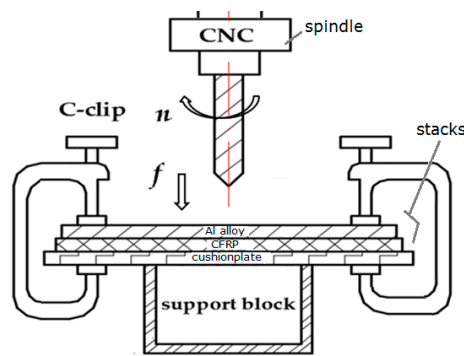


Figure 1. The manufacturing schematic.

The hole manufacturing device is shown in Figure 2. The CNC machine tool (VMC850E, Shenyang Machine Tool Co., Ltd., Shenyang, China) was used to make holes in the CFRP and aluminum alloy stack material. Fixture clamps and positions of the stack material and the support block are also shown. The composite material is prone to burr, delamination, or tearing and other defects on the exit side. Thus, in the experimental scheme plans, a cushion plate with 3 mm thickness was used at the bottom of the composites to reduce the defects of holes. In addition, a program was used to control the spindle rotation speed of the CNC machine and make it a downward feed motion, which reduced the effect on the quality of holes.

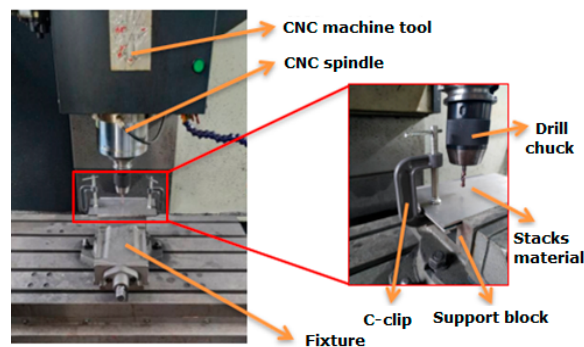


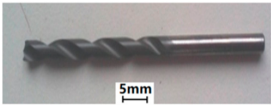
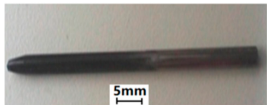
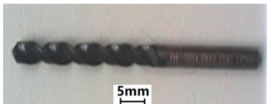
Figure 2. The manufacturing device.

2.2. The Process of Hole Manufacturing

In order to ensure the reliability of the experimental data, the CFRP materials before the experiment were carefully cut using special diamond cutters to ensure that there were no original defects. All experiments were conducted under the following conditions: (1) the integrity of the diamond layer on the drilling tool surface was checked; (2) the CNC machine was verified to be in good working condition; (3) the stack material was clamped by the C-clip without gaps and reliably positioned by the vise.

The structure parameters and materials of the tool have a great influence on the quality of holes. Therefore, before the experimental analysis of the stack material, the drilling effects of four kinds of cutting tools, including a three-pointed two-edge drill, double-edge drill, reamer drill, and octahedral composite drill, were firstly compared on the CFRP material to check the quality of hole-making. The four types of drilling tools are shown in Table 1. The hole diameter was 4.8 mm, the average hole-making distance was 12 mm, and the count was 20. A total of 20 holes with one cutter was the basic requirement. For the 140 × 140 mm T300 CFRP with 3 mm thickness, basic experimental research was performed on the CNC machines. The corresponding drilling effect diagrams are shown in Figure 3.

Table 1. Four types of drilling tool ($\Phi 4.8$ mm).

Drill Bit	Appearance Picture	Drill Bit	Appearance Picture
Three-pointed two-edged drill		Reamer drill	
Double-edged drill		Octahedral composite drill	

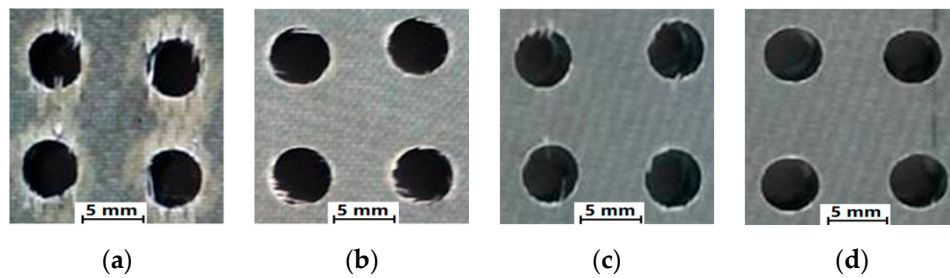


Figure 3. The appearance of the hole exit using the four types of tools: (a) three-pointed two-edged drill; (b) double-edged drill; (c) reamer drill; (d) octahedral composite drill.

It can be seen that the tearing defect in Figure 3a was significant, and the carbon fiber showed obvious tearing defects surrounding the hole. In Figure 3b,c, there were also carbon fiber burrs, but the tearing defect in the hole edge was not obvious. As a result, the effect of the octahedral composite drill was the best as shown in Figure 3d, and the quality of hole exit of all 20 holes met the requirements. Thus, the octahedral composite drill was chosen to manufacture all holes for further study.

In order to improve manufacturing quality of holes, cushion plates with 3 mm thickness made of pine, Al5051 sheet, and acrylonitrile butadiene styrene(ABS) plastic plate were selected for pre-experiments based on the previous experimental results. After that, the hole quality was compared. The experimental results are shown in Figure 4. It can be found that the ABS plastic cushion plate had the best effect on hole-making. Thus, the ABS plastic cushion plate with 3 mm thickness was used for all holes in further experimental studies with the CFRP at the bottom of the stacks.

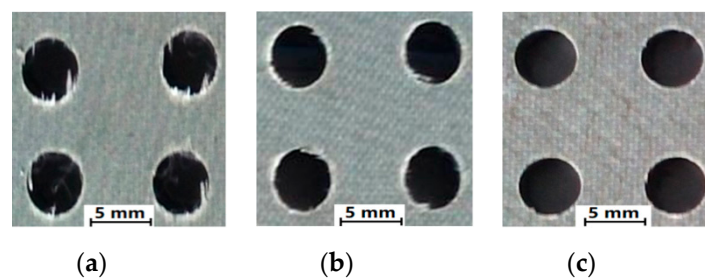


Figure 4. The appearance of the hole exit using three types of cushion plates: (a) pine; (b) Al5051; (c) ABS plastic.

In this paper, the stack materials composed of T300 CFRP (thickness 3 mm) and 7050-T7 (thickness 2 mm) Al alloy were studied. The main defects for holes of CFRP were burrs, delamination, and tearing. The hole-making defects of CFRP were the main research object, and experimental research and prediction analysis were carried out. Four parameters of feed rate (0.005–0.06 mm/r), spindle speed (2000–9000 r/min), drilling diameter (3–8 mm), and cushion plate were taken as the input layer parameters to study the effect of manufacturing holes. Four stack types (CFRP/Al, Al/CFRP,

Al/CFRP/Al, and CFRP/Al/CFRP) were studied. The 140×140 mm area in the middle of the support block was the hole-making area of the stack material. The average hole-making distance was 20 mm and the count was 20. Each set of hole-making experiments used a new tool to manufacture 20 holes, as well as for chip suction and natural cooling. After each hole was manufactured, the interval was 30 s for cooling the tool, before the next hole was manufactured for a complete set of experiments. In the experiments, the effects of drilling position difference were ignored. In addition, the wear of the cutting edge on hole-making was not considered in this study, because the maximum number of holes made by the new tool was not more than 20. For different combinations of process parameters, a total number of 161 sets of experiments were completed. Tests No. 1–152 were used as training samples and tests No. 153–161 were used as prediction samples.

2.3. The Quality Inspection of Holes

It was found that the edge damage of each hole was caused by delamination, tearing, slagging, etc. The quality evaluation criteria of manufacturing holes mainly referred to the requirements of an aviation company. A schematic diagram of the defect area at the edge of the hole is shown in Figure 5. If the degree of defect is within the range shown in Table 2, it is qualified and no further processing is required.

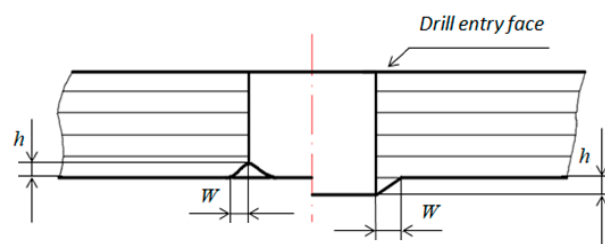


Figure 5. Defect range for hole-making in carbon fiber-reinforced plastic (CFRP).

Table 2. Defect criteria for hole-making in CFRP.

Hole Diameter	h (Maximum)	W (Maximum)
3.18 mm	0.36 mm	1.27 mm
3.97 mm	0.36 mm	2.54 mm
4.76 mm	0.36 mm	2.54 mm
6.35 mm	0.36 mm	2.54 mm
7.94 mm	0.36 mm	3.04 mm

The A-scan determines the orientation and size of the defect by measuring the amplitude of the echo signal and the position of the transmitting transducer [14]. The characteristics and testing requirements of carbon fiber composites were considered, and the A-scan ultrasonic detector was used for scanning detection in this study. The exit surface morphology of the sample was observed using an ultra-depth electron microscope (VHX-500F) produced by Japan Keyence. In the verification test, a three-jaw internal micrometer (accuracy 0.0001 mm) was used to measure the hole diameter, and the SJ-210 surface roughness measuring instrument from Japan's Mitutoyo was used to measure roughness Ra.

3. BP Neural Network Prediction for the Tear Number of Hole

3.1. Introduction of BP Neural Network

The BP neural network has good self-learning, adaptive, and generalization capabilities [15]. The learning process consists of two procedures: forward propagation of signal and back propagation of error. When the signal propagates forward, the input sample is passed in from the input layer. After

being processed by neurons in each hidden layer, the input sample is transferred to the output layer. Finally, the result is obtained. If the result is inconsistent with the expected output, it is transferred to the reverse propagation phase. The error back propagation is that the output error was layer-by-layer back-transferred to the input layer through the hidden layer, and the error was distributed to all the units of each layer and used as the basis for adjusting the weights of each unit. By modifying the weights of each element, the error was reduced by the gradient [16]. This process was repeated over and over again until the error in the network output was reduced to an acceptable level.

3.2. Establishment of Neural Network Model

An 8–14–1 three-layer topology was used to construct a neural network model for predicting the drilling quality, as shown in Figure 6. The topology of the BP neural network model usually includes an input layer, hidden layer, and output layer [17]. The input layer mainly receives external data and information, the hidden layer is calculated using various functional relationships, and the output layer is mainly used to carry out the calculation conclusions and give prediction results.

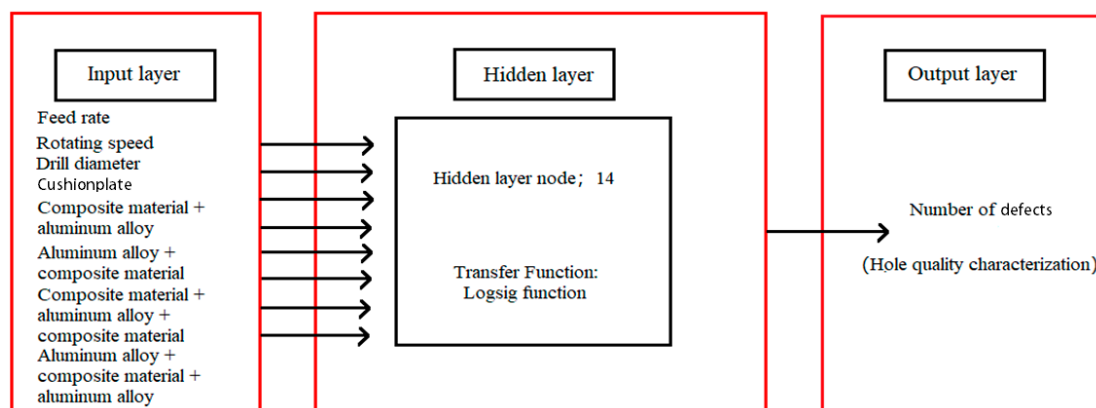


Figure 6. The three-layer topology of the prediction model.

3.3. Selection of Hidden Layer Nodes

The selection of hidden layer nodes has great influence on the prediction accuracy of the BP neural network [18]. The prediction experiment was carried out by cut-and-trial. The results are shown in Table 3. The error in the table is the sum of the errors between the theoretical prediction data and the actual data.

Table 3. The error of hidden nodes.

Node	7	8	9	10	11	12	13	14	15	16	17
Error	325	197	123	62	167	135	100	28	57	84	224

If the quantity of hidden layer nodes is too small, the complex mapping relationship cannot be established by the BP neural network, and the error of network prediction is relatively larger. On the other hand, when the number of hidden layer nodes is too high, the learning time will increase, which may cause the prediction of training samples to be accurate, but the error of prediction samples will be larger. In general, the error of network prediction decreases and then increases with the increase in the number of nodes. According to Table 3, when 14 hidden layer nodes were selected, the error was the minimum.

3.4. Prediction-Influencing Factors of BP Neural Network

As shown in Table 4, the first row constitutes the process parameters and the composition of stack materials. In the composition column, the order from left to right represents the stacking order of

materials from top to bottom. A value of 1 indicates that it was carried out and a value of 0 indicates that it was not used. Similarly, in the “cushion plate” column, a value of 1 indicates that it was carried out with an ABS cushion plate of 3 mm thickness, while a value of 0 indicates that it was not used.

Table 4. Input vector level.

Input Vector	Feed Rate (mm/r)	Spindle Speed (r/min)	Drilling Diameter (mm)	CFRP (3 mm) (Y1, N0)	Al (2 mm) (Y1, N0)	CFRP (3 mm) (Y1, N0)	Al (2 mm) (Y1, N0)	Cushion Plate (Y1, N0)
Level I	0.007	3000	3.26	0/1	0/1	0/1	0/1	0/1
Level II	0.02	5000	4.81	0/1	0/1	0/1	0/1	0/1
Level III	0.04	7000	7.92	0/1	0/1	0/1	0/1	0/1

A total of eight input vectors, 14 hidden layer nodes, and one output vector were substituted into the toolbox of the Matlab neural network. The BP neural network created by the newff function was used as the prediction model. The steps were as follows: (1) the transfer function of input layer nodes of the model was tansig ($y = 2/[1 + \exp(-2x)] - 1$); (2) the transfer function of the implicit layer node was logsig ($y = 1/[1 + \exp(-x)]$), and the transfer function of the output layer node selected purelin ($y = x$); (3) the weight training function selected the trainlm function, which uses the Levenberg–Marquardt optimization algorithm (least squares algorithm).

4. Training and Verification Experiment of BP Neural Network Model

4.1. Model Training

Only a trained neural network model can predict the defect number of holes. Figure 7 shows the training diagram of the neural network model. After undergoing an error correction of 170 steps, the error was reduced to 0.00016882, and the regression fit was 0.99978. The steps were as follows: (1) training data and prediction data were loaded and normalized; (2) the network structure was built through the newff function, the number of training steps was set at 170, and the error target was 0.0001. Then, training data were trained online; (3) the trained grid was used to fit the training data and forecast data, and then the fitting results were reversely normalized; (4) at last, the training and predict data were compared with the actual data.

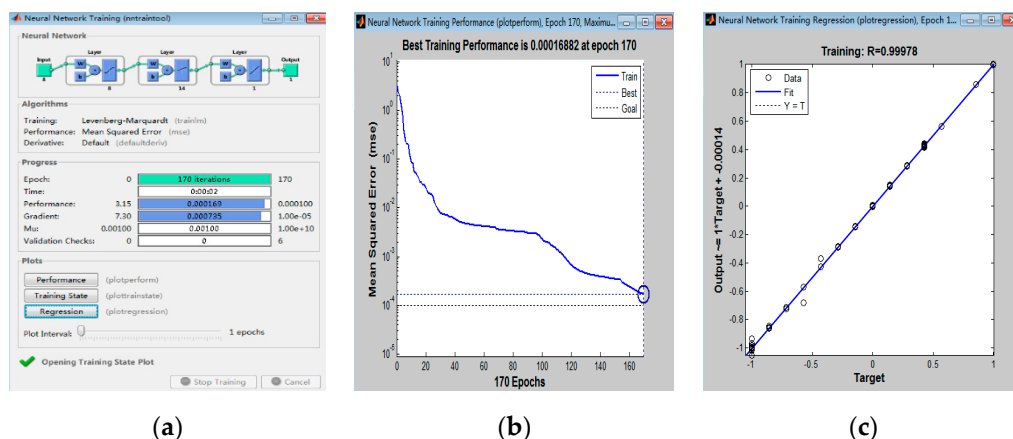


Figure 7. Training diagram: (a) process; (b) mean square error; (c) regression fitting.

4.2. Results Calculation

According to the rounding principle, the error of the fitting results was as shown in Figure 8.

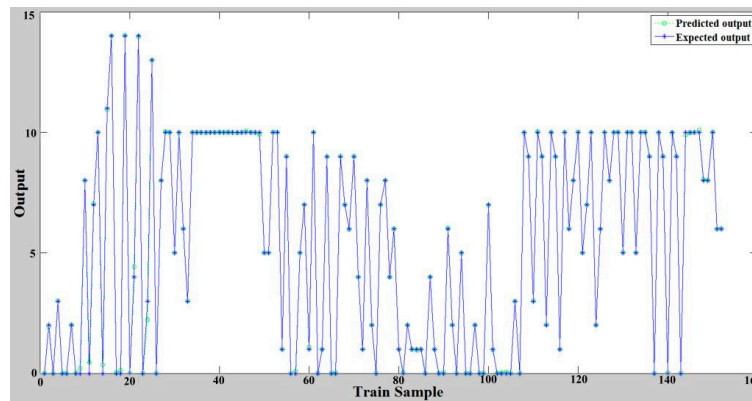


Figure 8. The fitting result diagram of training samples.

In Figure 8, * represents that the expected value is equivalent to the actual experimental result, and ° represents that the predicted value is equivalent to the theoretical value. The fit between the expected value of the tearing number and the predicted value was good and most samples were almost coincident. The magnitude of training sample fitting error was 10^{-2} – 10^{-5} , and a small number of samples had an error of 10^{-1} . Within the magnitude, the maximum error was 0.78, which appeared in sample No. 24.

The process parameters of CFRP/Al/CFRP were predicted by the BP neural network model. The process parameters included the feed rate (0.04 mm/r), spindle speed (3000 r/min, 5000 r/min, 7000 r/min), drilling diameter (3.26 mm, 4.81 mm, 7.92 mm), and the ABS cushion plate with thickness of 3 mm. The predicted number of defective holes was consistent with the number of actual defects in 20 samples obtained from the test. The data are shown in Table 5.

Table 5. The comparison of predicted and actual values.

Test No.	Feed Rate (mm/r)	Spindle Speed (r/min)	Drilling Diameter (mm)	CFRP (3 mm) (Y1, N0)	Al (2 mm) (Y1, N0)	CFRP (3 mm) (Y1, N0)	Cushion Plate (Y1, N0)	Actual Number of Defects	Prediction Number of Defects	Absolute Value of Error
153	0.04	3000	3.26	1	1	1	1	10	7	3
154	0.04	3000	4.81	1	1	1	1	8	6	2
155	0.04	3000	7.92	1	1	1	1	10	9	1
156	0.04	5000	3.26	1	1	1	1	10	9	1
157	0.04	5000	4.81	1	1	1	1	5	6	1
158	0.04	5000	7.92	1	1	1	1	0	0	0
159	0.04	7000	3.26	1	1	1	1	10	14	4
160	0.04	7000	4.81	1	1	1	1	8	12	4
161	0.04	7000	7.92	1	1	1	1	5	5	0

It can be seen from Table 5 that the maximal error of prediction was 4, which appeared in tests No. 159 and No. 160. The minimum error of prediction was at least 0, which appeared in tests No. 158 and No. 161. It is known from the data in Figure 9 and Table 5 that the prediction results were consistent with the trend of the experimental results. However, the error of some separate samples was larger in the prediction results. The prediction model was based on the training samples, but the process parameters of tests No. 153–No. 161 did not exist in the training samples, and the prediction model was still based on the training samples during the prediction process, which caused a larger error. However, this error can be reduced by increasing the number of training samples. The same principle can also be used to predict the optimized hole-making processes for CFRP/Al, Al/CFRP, and Al/CFRP/Al.

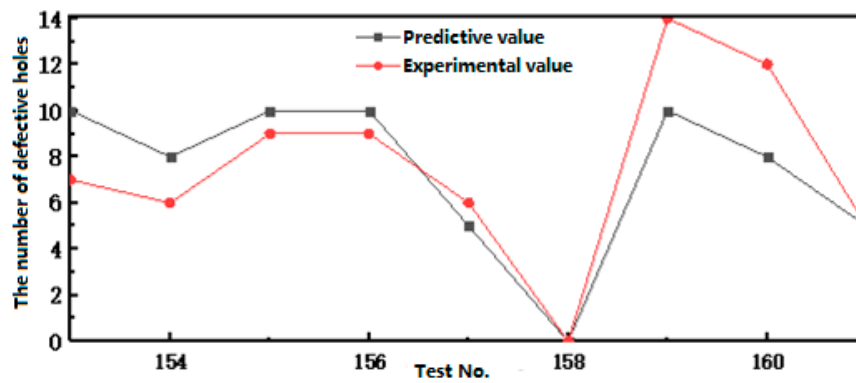


Figure 9. The comparison of predicted and expected values.

As shown in Figure 9, the prediction curve of the number of defective holes was similar to the trend of the experimental curve, but the prediction errors of samples No. 159 and No. 160 were larger.

4.3. Model Verification

The exit surface morphology was observed by ultra-depth electron microscopy (VHX-500F). The accuracy of the BP neural network in predicting drilling quality was verified by comparing the surface topography. Firstly, the edge morphology was observed when the hole was magnified 100× and the measuring scale was 300 μm. Then, the inner surface topography of the holes was observed when the hole was magnified 300× and the measuring scale was 150 μm. The results of sample No. 155 and sample No. 158 are shown in Figure 10; through a comparison, it can be found that the tearing defects at the hole exit and the delamination defect on the inner surface of the hole were obvious.

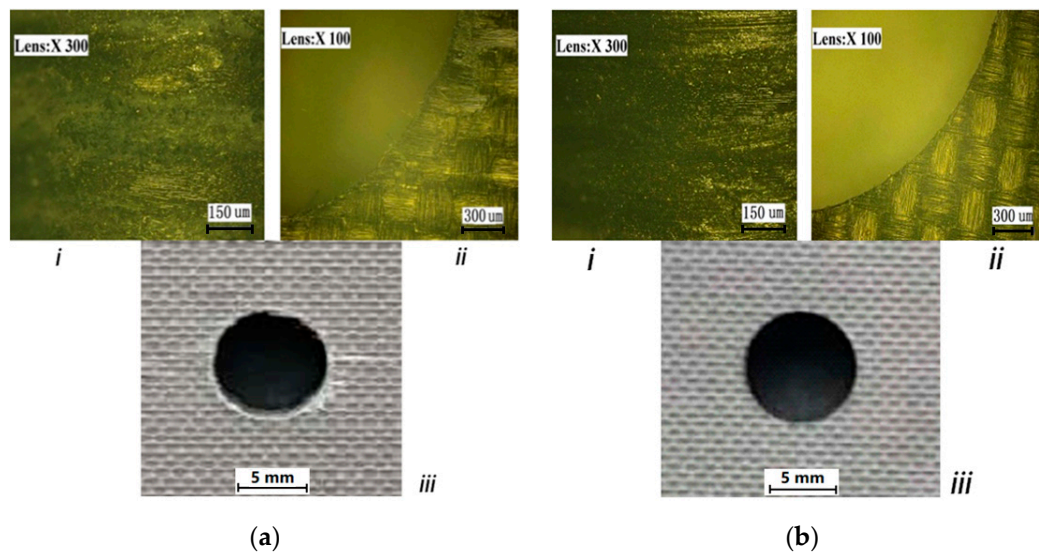


Figure 10. Surface topography of CFRP samples: (a) sample No. 155; (b) sample No. 158. i—interior surface morphology; ii—edge morphology; iii—exit appearance.

The delamination generated during drilling has a certain functional relationship with the drilling thrust force. When the drilling tool approaches the plane of exit, the stiffness of the cutting delamination cannot withstand the axial thrust force. Thus, the material around the bottom plate layer drilling may be separated and removed from the junction of the internal laminates. The circular plate model for hierarchical analysis is shown in Figure 11 and the defect range of the hole surface is shown in Figure 12.

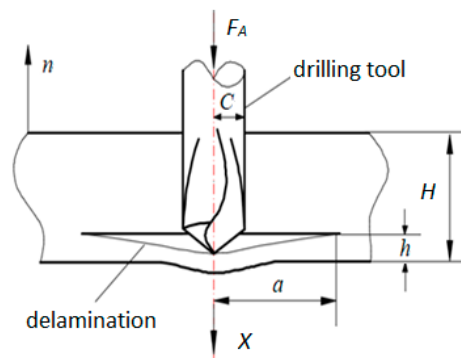


Figure 11. Circular plate model for drilling CFRP.

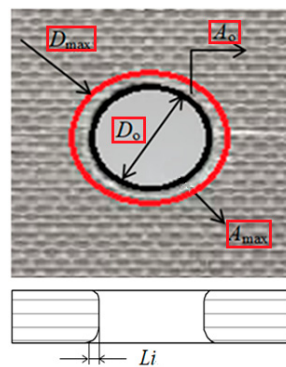


Figure 12. The defect diagram of tearing.

As shown in Figure 11, a drill bit with a radius C applies a load to the center of the circular plate. F_A denotes the thrust, X denotes the displacement, H is the thickness, h is the thickness of the uncut layer under the tool, and a is the radius of the delamination range. Assuming that the composite laminate of each layer is isotropic, Equation (1) can be obtained according to the linear elastic fracture mechanics and the law of conservation of energy [19].

$$G_{IC}dA = F_A X - dU, \tag{1}$$

where: G_{IC} donates critical crack propagation energy per unit area, which is constant as a function of strain rate [20], $dA = 2\pi a \cdot da$ denotes the growth area of the delamination, and U donates the stored strain energy, which can be calculated using the classical thin plate theory [21].

$$U = \frac{8\pi M X^2}{a^2}, \tag{2}$$

where M donates the stiffness of CFRP material per unit width, and the expression is

$$M = \frac{E h^3}{12(1 - \nu^2)}, \tag{3}$$

where E denotes Young's modulus, ν denotes the Poisson's ratio of CFRP material, and the displacement X is

$$X = \frac{F_A a^2}{12\pi M}. \tag{4}$$

Combining the above formulas, the drilling thrust at the beginning of crack propagation [22] can be expressed as

$$F_A = \pi \left[\frac{8G_{IC}Eh^3}{3(1-\nu^2)} \right]^{\frac{1}{2}}, \tag{5}$$

where h can be calculated by $\frac{\partial F_A}{\partial h} = 0$.

As shown in Figure 12, D_0 denotes the drill diameter (mm), D_{max} denotes the maximum diameter of the tearing range (mm), A_{max} denotes the area of the tearing defect (mm²), and A_0 denotes the area formed by ΦD_0 . The stratification adjustment factor F_{da} can be expressed as

$$F_{da} = \alpha \frac{D_{max}}{D_0} + \beta \frac{A_{max}}{A_0}, \tag{6}$$

where α and β are the weighting factor ($\alpha + \beta = 1$).

When the tool drilled out the surface of the composite material, the composite material was pressed by the axial force and the blade, and cracks were formed at the edge of the holes at the initial stage [23]. As the process continued, the thickness of the material to be cut became thinner, the rigidity decreased, and the cracks gradually expanded; the fiber of surface at the center of the drill bit fractured. Under the action of friction force, greater shear stress was generated at the outlet of the work piece. Finally, the crack formed a tearing range, which is the most common defect in the hole-making process. The drilling thrust required by octahedral composite drilling is relatively small; thus, the occurrence of delamination and tearing of holes was also relatively low after the experimental studies and theoretical analysis. However, the geometric parameters of the drilling tools, which affect the size of the drilling force under the same cutting conditions, also affect the generation of delamination defect.

During the hole-making process, the chipped, fracture, or excessive wear of the cutting edge of drilling tool will cause the working noise of the CNC equipment to increase greatly; the CFRP material will overheat, and the axial force will increase. Therefore, when using the process parameters of the BP neural network prediction model to make holes in stack materials, these abnormal working phenomena must be paid attention to. Based on the BP neural network prediction model, the manufacturing quality of the holes for stack materials composed of T300 CFRP and 7050-T7 Al alloy with different diameter and types was predicted, and the optimal hole-making process parameters were obtained. Some optimization parameters applied to normal production are shown in Table 6, and the total number of holes generated was more than 1000.

Table 6. Some applied optimization parameters.

Optimization No.	Feed Rate (mm/t)	Spindle Speed (r/min)	Drilling Diameter (mm)	CFRP (3 mm) (Y1, N0)	Al (2 mm) (Y1, N0)	CFRP (3 mm) (Y1, N0)	Al (2 mm) (Y1, N0)	Cushion Plate (Y1, N0)	Prediction Number of Defects
P1001	0.007	5500	6.35	1	1	0	0	0	0
P1002	0.02	3300	4.83	0	1	1	0	1	0
P1003	0.04	7000	3.26	0	1	1	1	0	0
P1004	0.007	7000	7.94	1	1	1	0	1	0

In practical applications, the qualified rate of manufactured holes ($\Phi 3$ – $\Phi 8$ mm) is as high as 97%. According to the measurement of holes, other technical indicators are also very good. The highest hole diameter tolerance of CFRP material can meet the requirements of H9, and the surface roughness of most holes is lower than Ra 3.2, which greatly shortens the development cycle of new hole-making processes and improves the manufacturing quality of stack materials composed of T300 CFRP (thickness 3 mm) and 7050-T7 (thickness 2 mm) Al alloy.

5. Conclusions

The BP neural network algorithm was used to predict the manufacturing quality of holes in stack materials made of T300 CFRP and 7050-T7 Al alloy superimposed in this study. An 8–14–1

three-layer topology model was designed, and a prediction model was established according to different hole-making processes in the four types of stack material by using the same drilling tool. Then, the training results were compared with the experimental data. Finally, the prediction model was verified by theoretical analysis and experimental results. The main conclusions are summarized as follows:

- (1) The octahedral composite drill and ABS plastic cushion plate with 3 mm thickness were firstly chosen to manufacture all holes. The parameters of input layer were the feed rate, spindle speed, drilling diameter, and cushion plate, with CFRP/Al, Al/CFRP, Al/CFRP/Al, and CFRP/Al/CFRP composites. The output layer parameter was the number of defective holes.
- (2) According to the BP neural network prediction model with 8–14–1 three-layer topology, which underwent error correction of 170 steps, the error was reduced to 0.00016882, the regression fit was 0.99978, and the magnitude of training sample fitting error was about 10^{-2} – 10^{-5} .
- (3) Based on the BP neural network prediction model, the optimized processes of hole-making were obtained. The qualified rate of manufactured holes ($\Phi 3$ – $\Phi 8$ mm) for stack materials composed of T300 CFRP (thickness 3 mm) and 7050-T7 (thickness 2 mm) Al alloy reached 97%.

Author Contributions: Overall program guidance, W.L.; program implementation and analysis, A.J.; experimental research and testing, G.Z. and B.L. All authors read and agree to the published version of the manuscript.

Funding: The paper was supported by “High-end CNC machine tools and basic manufacturing equipment” (2016ZX04002005) of National Major Science and Technology Projects, China, by the Natural Science Foundation of Liaoning Province (2019-ZD-0029), and by the University of Science and Technology Liaoning Talent Project Grants (601011507-32).

Conflicts of Interest: The authors declare no conflicts of interest.

References

1. Chen, Y.; Ge, E.; Fu, Y.; Su, H.; Xu, J. Review and prospect of drilling technologies for carbon fiber reinforced polymer. *Acta Mater. Compos. Sin.* **2015**, *32*, 301–316.
2. Qiu, J.; Chen, J.; Hao, H. Study on the technology of low damage ultrasonic vibration drilling of CFRP. *Mech. Sci. Technol. Aerosp. Eng.* **2019**, *38*, 1–8.
3. Shutao, H.; Haotao, W.Z.; Pan, Z. Finite element analysis on drilling defects of carbon fiber reinforced plastic and aluminum stacks. *J. Mater. Sci. Eng.* **2019**, *37*, 493–500.
4. Dharan, C.K.H.; Won, M.S. Machining parameters for an intelligent machining system for composite laminates. *Int. J. Mach. Tools Manuf.* **2000**, *40*, 415–426. [[CrossRef](#)]
5. Davim, J.P.; Reis, P. Study of delamination in drilling carbon fiber reinforced plastics (CFRP) using design experiments. *Compos. Struct.* **2003**, *59*, 481–487. [[CrossRef](#)]
6. Mubarak, A.; Joshi, S.C.; Hameed, S.M.T. Palliatives for low velocity impact damage in composite laminates. *Adv. Mater. Sci. Eng.* **2017**, *2017*, 1–16.
7. Hocheng, H.; Tsao, C.C. Comprehensive analysis of delamination in drilling of composite materials with various drill bits. *J. Mater. Process. Technol.* **2003**, *140*, 335–339. [[CrossRef](#)]
8. Omar, O.E.E.K.; El-Wardany, T.; Ng, E.; Elbestawi, M.A. An improved cutting force and surface topography prediction model in end milling. *Int. J. Mach. Tools Manuf.* **2007**, *47*, 1263–1275. [[CrossRef](#)]
9. Kalla, D.; Sheikh-Ahmad, J.; Twomey, J. Prediction of cutting forces in helical end milling fiber reinforced polymers. *Int. J. Mach. Tools Manuf.* **2010**, *50*, 882–891. [[CrossRef](#)]
10. Karpat, Y.; Er, B.; Bahtiyar, O. Drilling thick fabric woven cfrp laminates with double point angle drills. *J. Mater. Process. Technol.* **2012**, *212*, 2117–2127. [[CrossRef](#)]
11. Chen, T.; Wang, D.Y.; Gao, F.; Liu, X.L. Experimental study on milling cfrp with staggered pcd cutter. *Appl. Sci.* **2017**, *7*, 934. [[CrossRef](#)]
12. Ugoenemuoh, E.; SherifEl-Gizawy, A. Optimal neural network model for characterization of process-induced damage in drilling carbon fiber reinforced epoxy composites. *Mach. Sci. Technol.* **2003**, *7*, 389–400.

13. Karnik, S.R.; Gaitonde, V.N.; Rubio, J.C.; Correia, A.E.; Abrão, A.M.; Davim, J.P. Delamination analysis in high speed drilling of carbon fiber reinforced plastics (CFRP) using artificial neural network model. *Mater. Des.* **2008**, *29*, 1768–1776. [[CrossRef](#)]
14. Wang, F.S.; Ma, X.T.; Zhang, Y.; Jia, S.Q. Lightning damage testing of aircraft composite-reinforced panels and its metal protection structures. *Appl. Sci.* **2018**, *8*, 1791. [[CrossRef](#)]
15. Ding, S.; Su, C.; Yu, J. An optimizing bp neural network algorithm based on genetic algorithm. *Artif. Intell. Rev.* **2011**, *36*, 153–162. [[CrossRef](#)]
16. Li, J.; Cheng, J.H.; Shi, J.Y.; Huang, F. *Brief Introduction of Back Propagation (BP) Neural Network Algorithm and Its Improvement*; Springer: Berlin/Heidelberg, Germany, 2012. [[CrossRef](#)]
17. Geng, X.G.; Lu, S.Z.; Jiang, M.S.; Sui, Q.; Lv, S.; Xiao, H.; Jia, Y.; Jia, L. Research on fbg-based cfrp structural damage identification using bp neural network. *Photon. Sens.* **2018**, *8*, 168–175. [[CrossRef](#)]
18. Zou, W.; Li, Y.; Tang, A. Effects of the number of hidden nodes used in a structured-based neural network on the reliability of image classification. *Neural Comput. Appl.* **2009**, *18*, 249–260. [[CrossRef](#)]
19. Rahme, P.; Landon, Y.; Lagarrigue, P.; Piquet, R.; Lachaud, F.; Marguet, B.; Bourriquet, J.; Le Roy, C. Drilling of thick composite structures state of the art. *SAE Int.* **2006**. [[CrossRef](#)]
20. Saghizadeh, H.; Dharan, C.K.H. Delamination fracture toughness of graphite and Aramid epoxy composites. *ASME J. Eng. Mater. Technol.* **1986**, *108*, 290–295. [[CrossRef](#)]
21. Childs, T.H.C.; Dirikolu, M.H.; Maekawa, K. Modelling of friction in the simulation of metal machining. *Tribol. Interface Eng.* **1998**, *34*, 337–346.
22. Hocheng, H.; Dharan, C.K.H. Delamination during drilling in composite laminates. *ASME J. Eng. Ind.* **1990**, *112*, 236–239. [[CrossRef](#)]
23. An, Q.; Cai, X.; Xu, J.; Chen, M. Experimental investigation on drilling of high strength T800s/250F CFRP with twist and dagger drill bits. *Int. J. Abras. Technol.* **2014**, *6*, 183–196. [[CrossRef](#)]



© 2020 by the authors. Licensee MDPI, Basel, Switzerland. This article is an open access article distributed under the terms and conditions of the Creative Commons Attribution (CC BY) license (<http://creativecommons.org/licenses/by/4.0/>).